Thermodynamic Bounds on Generalized Transport: From Single-Molecule to Bulk Observables

Cai Dieball and Aljaž Godec*

Mathematical bioPhysics Group, Max Planck Institute for Multidisciplinary Sciences, 37077 Göttingen, Germany

(Received 29 February 2024; revised 29 May 2024; accepted 11 July 2024; published 5 August 2024)

We prove that the transport of any differentiable scalar observable in d-dimensional nonequilibrium systems is bounded from above by the total entropy production scaled by the amount the observation "stretches" microscopic coordinates. The result—a time-integrated generalized speed limit—reflects the thermodynamic cost of transport of observables, and places underdamped and overdamped stochastic dynamics on equal footing with deterministic motion. Our work allows for stochastic thermodynamics to make contact with bulk experiments, and fills an important gap in thermodynamic inference, since microscopic dynamics is, at least for short times, underdamped. Requiring only averages but not sample-to-sample fluctuations, the proven transport bound is practical and applicable not only to single-molecule but also bulk experiments where only averages are observed, which we demonstrate by examples. Our results may facilitate thermodynamic inference on molecular machines without an obvious directionality from bulk observations of transients probed, e.g., in time-resolved x-ray scattering.

DOI: 10.1103/PhysRevLett.133.067101

A complete thermodynamic characterization and understanding of systems driven far from equilibrium remains elusive. Central to nonequilibrium thermodynamics is the total entropy production ΔS_{tot}, which reflects the displacement from equilibrium [1]. ΔS_{tot} embodies the entropy change in both the system and the environment coupled to it and is a measure of the violation of time-reversal symmetry [1,2]. Most importantly, the *thermodynamic cost* of nonequilibrium processes (stationary, transient, or even explicitly time-dependent) at temperature T is in fact $T\Delta S_{\mathrm{tot}}$, which can thus be seen as the "counterpart" of free energy in equilibrium. The total entropy production allows, for example, to quantify the efficiency of molecular motors [3–5] and gain insight into the energetic budget of human red blood cells [6]. While most works focus on nonequilibrium steady-state (NESS) dynamics, transient processes that approach equilibrium states such as, e.g., protein folding [7–15] or thermal relaxation [16], are also characterized by $T\Delta S_{\mathrm{tot}}$, which then corresponds to an excess free energy [16–19]. Even more involved are transients toward NESS, relevant in e.g., the packaging of viral DNA [20], red blood cell flickering [21], enzymatically facilitated topological relaxation of DNA [22], or nanoparticle model systems for interrogating the fundamental laws of stochastic thermodynamics [23].

Despite its importance, the inference of ΔS_{tot} from experimental observations is far from simple, as it requires access to *all* dissipative degrees of freedom is the system, which is typically precluded by the fact that one only has access to some observable. Notably, neither the microscopic dynamics nor the projection underlying the observable are typically known, and often one can only observe transients.

To overcome these intrinsic limitations of experiments, diverse bounds (i.e., inequalities) on the entropy production have been derived, in particular thermodynamic uncertainty relations (TURs) [24–37] and speed limits [38–48]. Such bounds provide conceptual insight about manifestations of irreversible behavior, and from a practical perspective they allow to infer a bound on ΔS_{tot} from measured trajectories, more precisely from the sample-to-sample fluctuations or speed of observables.

These results remain incomplete from several perspectives. First, their validity typically hinges on the assumption that the microscopic dynamics is overdamped or even a Markov-jump process. This is unsatisfactory because microscopic dynamics is, at least on short timescales, underdamped and the TUR does *not* hold for underdamped dynamics [49] (see, however, progress in [50–53] and recently [54]). Similarly, thermodynamic speed limits have so far seemingly not been derived for underdamped dynamics. While inertial effects may not be important in colloidal systems [55], they are indeed relevant for, e.g., protein dynamics [56–59], and are known to invalidate overdamped theories even on long timescales [49]. Even

*Contact author: agodec@mpinat.mpg.de

the basic formulation of path-wise thermodynamics of inertial systems is fundamentally different, and in the analysis of densities or integrals over stochastic trajectories one cannot eliminate short-time inertial effects. Second, dissipative processes are often, especially in molecular machines without an obvious directionality (e.g., molecular chaperones [60]), mediated by intricate collective (and often fast) open-close motions visible in transients that are difficult to resolve even with advanced single-molecule techniques [61]. Experiments providing more detailed structural information, such as time-resolved x-ray scattering techniques [7–10,12–15], are available, but probe bulk behavior for which the existing bounds do not apply. There is thus a pressing need to close the gaps and to cover underdamped dynamics and tap into bulk observations.

Here, we present thermodynamic bounds on the generalized transport of observables in systems evolving according to (generally time-inhomogeneous) overdamped, underdamped, or even deterministic dynamics, all treated on an equal footing, generalizing existing results on transport [4,46]. Technically, the results may be classified as a time-integrated version of generalized speed limits and bring several conceptual and practical advantages. As a demonstration, we use the bounds for thermodynamic inference based on both single-molecule and bulk (e.g., scattering) observables.

Rationale—Consider the simplest case of a Newtonian particle with position x_τ and velocity v_τ at time τ dragged through a viscous medium against the (Stokes) friction force $F_\gamma = -\gamma v_\tau$ with friction constant γ causing a transfer of energy into the medium. The dissipated heat between times 0 and t is $\Delta Q_\gamma = \gamma \int_0^t v_\tau dx_\tau = \gamma \int_0^t v_\tau^2 d\tau$ and gives rise to entropy production in the medium [1]. Since deterministic dynamics does not produce entropy otherwise, we have $T\Delta S_{\rm tot} = \Delta Q_\gamma$ in $\tau \in [0,t]$. This imposes a thermodynamic bound on transport via the Cauchy-Schwarz inequality $(x_t - x_0)^2 = (\int_0^t v_\tau 1 d\tau)^2 \leq \int_0^t v_\tau^2 d\tau \int_0^t 1^2 d\tau'$, yielding $T\Delta S_{\rm tot} \geq \gamma (x_t - x_0)^2/t$ with equality for constant velocity. Therefore, for given t and γ a minimum energy input ΔQ_γ is required to achieve a displacement $x_t - x_0$. The intuition that transport requires dissipation extends to general dynamics and scalar observables as follows.

Main result—The transport of any differentiable scalar observable $z_\tau \equiv z(\mathbf{x}_\tau, \tau)$ [see Ref. [62] for $z_\tau \equiv z(\mathbf{x}_\tau, \mathbf{v}_\tau, \tau)$] on a time interval $[0,t]$ in d-dimensional generally underdamped and time-inhomogeneous dynamics $(\mathbf{x}_\tau, \mathbf{v}_\tau)$ is bounded from above by $T\Delta S_{\rm tot}$ as

$$T\Delta S_{\rm tot} \geq \frac{\langle z_t - z_0 - \int_0^t \partial_\tau z_\tau d\tau \rangle^2}{t\mathcal{D}^z(t)}$$
$$\mathcal{D}^z(t) \equiv \frac{1}{t}\int_0^t \langle [\nabla_{\mathbf{x}} z_\tau]^T \boldsymbol{\gamma}^{-1}(\tau) \nabla_{\mathbf{x}} z_\tau \rangle d\tau, \qquad (1)$$

where $\boldsymbol{\gamma}$ is a positive definite, possibly time-dependent, symmetric friction matrix, $\langle\cdot\rangle$ denotes an ensemble average over nonstationary trajectories, and $\mathcal{D}^z(t)$ is a fluctuation-scale function of the observable that determines how much the observation z *stretches* microscopic coordinates $\mathbf{x}$. While $\Delta S_{\rm tot}$ for stochastic dynamics differs from $\Delta Q_\gamma/T$, the bound (1) remains valid in the whole spectrum from Newtonian to underdamped and overdamped stochastic dynamics. The inequality saturates for $\nabla_{\mathbf{x}} z_\tau = c\boldsymbol{\gamma}\boldsymbol{\nu}(\mathbf{x}, \mathbf{v}, \tau)$ for any constant c and $\boldsymbol{\nu}$ defined in Eq. (4). Note that the application of Eq. (1) does *not* require knowledge of the parameters of the underlying motion. One only needs to infer the average in the numerator and $\mathcal{D}^z$. To infer the latter, different strategies are presented toward the end of the Letter.

Setting $z_\tau = x_\tau$ for $d = 1$, Eq. (1) includes the above deterministic case. In the overdamped limit, Eq. (1) complements the Benamou-Brenier formula that bounds transport in terms of a Wasserstein distance [48,67], and special cases of the bound correspond to existing overdamped speed limits [4,5,46] (in particular, Ref. [46] already contains an overdamped version of $\mathcal{D}^z$; see Ref. [62] for a detailed connection to the existing literature).

The bound (1) characterizes the thermodynamic cost of transport and may be employed in thermodynamic inference. By only requiring the mean but not sample-to-sample fluctuations, the bound (1) is simpler than the TUR and allows to infer $\Delta S_{\rm tot}$ from transients of bulk observables, probed, e.g., in time-resolved scattering experiments [7–10,12–15,68]. A disadvantage of this simplicity is that it is not useful for stationary states, unless they are translation invariant or periodic. The observable z_τ can represent a measured projection, whose functional form may be known (e.g., in x-ray scattering) or unknown (e.g., a reaction coordinate of a complex process). For optimization of thermodynamic inference z_τ may be chosen *a posteriori* and τ-dependent.

Outline—First we describe the setup and discuss different notions of $\Delta S_{\rm tot}$ from deterministic via underdamped to overdamped dynamics. Next we present examples in the context of single-molecule versus bulk x-ray scattering experiments, as well as higher-order transport in stochastic heat engines. We then explain how to interpret and infer the fluctuation-scale function $\mathcal{D}^z(t)$. We conclude with a perspective.

Setup—Let $\boldsymbol{\gamma}$, $\mathbf{m}$ be $d \times d$ positive definite, symmetric friction and mass matrices with square root $\sqrt{\boldsymbol{\gamma}}\sqrt{\boldsymbol{\gamma}}^T = \boldsymbol{\gamma}$. The full dynamics $\mathbf{x}_\tau, \mathbf{v}_\tau \in \mathbb{R}^d$ evolve according to [69]

$$d\mathbf{x}_\tau = \mathbf{v}_\tau d\tau$$
$$d\mathbf{v}_\tau = \mathbf{m}^{-1}\left[\mathbf{F}(\mathbf{x}_\tau, \tau)d\tau - \boldsymbol{\gamma}\mathbf{v}_\tau d\tau + \sqrt{2k_{\rm B}T\boldsymbol{\gamma}}d\mathbf{W}_\tau\right], \qquad (2)$$

which in the overdamped limit reduce to

$$d\mathbf{x}_\tau^{\rm od} = \boldsymbol{\gamma}^{-1}\mathbf{F}(\mathbf{x}_\tau^{\rm od}, \tau)d\tau + \sqrt{2k_{\rm B}T\boldsymbol{\gamma}^{-1}}d\mathbf{W}_\tau, \qquad (3)$$

where $\mathbf{F}(\mathbf{x},\tau)$ is a force field and $\mathbf{W}_\tau$ the d-dimensional Wiener process. We allow $\boldsymbol{\gamma}(\tau)$ [and later also $T(\tau)$] to depend on time but suppress this dependence to simplify notation. We define the *local mean velocity* $\boldsymbol{\nu}$ of the probability density ρ in phase space as $\boldsymbol{\nu}^{\text{Newton}} = \mathbf{v}$ and

$$\boldsymbol{\nu}(\mathbf{x},\mathbf{v},\tau) \equiv \mathbf{v} + \mathbf{m}^{-1} k_{\mathrm{B}} T \frac{\nabla_{\mathbf{v}} \rho(\mathbf{x},\mathbf{v},\tau)}{\rho(\mathbf{x},\mathbf{v},\tau)}$$
$$\boldsymbol{\nu}^{\text{od}}(\mathbf{x},\tau) \equiv \boldsymbol{\gamma}^{-1}\left[\mathbf{F}(\mathbf{x},\tau) - k_{\mathrm{B}} T \frac{\nabla_{\mathbf{x}} \rho^{\text{od}}(\mathbf{x},\tau)}{\rho^{\text{od}}(\mathbf{x},\tau)}\right]. \quad (4)$$

The definition for overdamped dynamics is standard [1], whereas in the underdamped setting $\boldsymbol{\nu}$ is only the "irreversible" part of the probability current divided by density [51]. Note that $\mathbf{v}_\tau = d\mathbf{x}_\tau/d\tau$ does not exist for overdamped dynamics as $\langle |d\mathbf{x}_\tau/d\tau| \rangle \to \infty$ for $d\tau \to 0$ but $\langle d\mathbf{x}_\tau \rangle/d\tau = \boldsymbol{\gamma}^{-1}\mathbf{F}(\mathbf{x},\tau)$ is well-behaved. The overdamped limit is loosely speaking obtained for $\boldsymbol{\gamma}^{-1}\mathbf{m} \to \mathbf{0}$, whereby details of this limit depend on $\mathbf{F}$ [70].

There are two differences between Newtonian and stochastic dynamics: (i) the energy exchange between system and bath counteracts friction, and (ii) changes in ρ give rise to a change in Gibbs entropy of a stochastic system, thus contributing to the total entropy production as $\Delta S_{\text{tot}} = \Delta S_{\text{sys}} + \Delta S_{\text{bath}}$. In all cases considered we can write the total entropy production as [1,2,51]

$$T\Delta S_{\text{tot}} = \int_0^t d\tau \langle \boldsymbol{\nu}^T(\mathbf{x}_\tau,\mathbf{v}_\tau,\tau)\boldsymbol{\gamma}\boldsymbol{\nu}(\mathbf{x}_\tau,\mathbf{v}_\tau,\tau)\rangle \geq 0. \quad (5)$$

Within this setup, an *educated guess* and stochastic calculus alongside the Cauchy-Schwarz inequality delivers the announced bound (1) (see proof in [62]).

Example 1: Colloid in displaced trap—Consider a bead trapped in a harmonic potential displaced from position 1 to 0 at time $\tau = 0$. Knowing γ and observing only the mean particle transport $\langle x_t - x_0 \rangle$ we infer the entropy production from Eq. (1) to be $T\Delta S_{\text{tot}} \geq T\Delta S_{\text{tot}}^{\text{bound}} \equiv \gamma \langle x_t - x_0 \rangle^2/t$. We inspect the quality of the bound, $Q \equiv \Delta S_{\text{tot}}^{\text{bound}}/\Delta S_{\text{tot}} \in [0,1]$, as a function of time (see Fig. 1). For underdamped dynamics Q tends to $3/4$ at short times due to inertia (see Ref. [62] for derivation). Using $z_\tau = x\nu(\tau)$ (for this example, ν turns out to be independent of x, v) we achieve saturation for all times, which is easily understood from our proof (see Ref. [62]). Saturation for this example was also achieved via the transient correlation TUR [37]. However, the present approach is expected to be numerically more stable and requires less statistics (see also Fig. S1 in [62]), since a determination of fluctuations and derivatives of observables is not required. Moreover, the simplest version $z_\tau = x_\tau$ outperforms the transient TUR for the simplest current $J_t = x_t - x_0$ [dashed line in Fig. 1(b)]. This may be interpreted as the magnitude of $x_t - x_0$ entering (1) being more relevant than its precision entering the TUR for this example. In contrast to the TUR [49], we also have the advantage that Eq. (1) holds for underdamped dynamics.

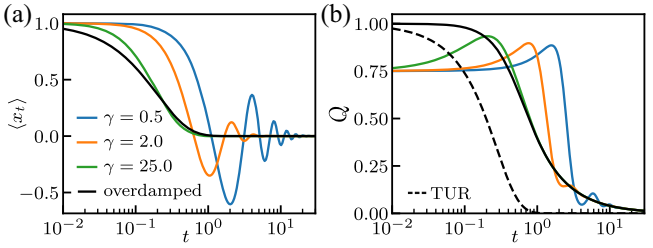

FIG. 1. Particle x_t in a harmonic trap displaced from $x = 1$ to $x = 0$ at time 0. (a) The particle's mean position $\langle x_0 \rangle = 1$ moves toward the new center of the trap, whereby oscillations occur for small damping. The probability density around $\langle x_\tau \rangle$ in this example is a Gaussian of constant width (see Ref. [62] for details and parameters). (b) Quality factor Q of the transport bound for the simplest observable $z_\tau = x_\tau$, and quality factor of the TUR for the current $J_t = x_t - x_0$ in the overdamped case. Full saturation $Q = 1$ at all times can be achieved for overdamped and underdamped dynamics as described below.

A disadvantage of Eq. (1) is that it is not useful for steady-state dynamics, since there $\langle z_t - z_0 \rangle = 0$. An exception is spatially periodic systems treated as NESS [3,4]. A particular example are overdamped Brownian clocks [71] where for given ΔS_{tot} the TUR limits *precision*, whereas Eq. (1) limits the magnitude of transport, i.e., the size of the clock. For a quantitative periodic example including comparisons to TURs see Fig. S1 in [62].

Example 2: Scattering experiments—Since Eq. (1) only requires averages, it is applicable beyond single-molecule probes to bulk experiments, i.e., experiments on samples of many molecules probing mean properties, e.g., scattering techniques. The recent surge in the development of time-resolved x-ray scattering on proteins [7–15] renders our bound particularly useful. Here, transients may be excited by a pressure [72,73] or temperature [74] quench, or one directly monitors slow kinetics [75]. One typically observes the structure factor $S(\mathbf{q}) \equiv (1/N)\sum_{j,k=1}^N \langle e^{-i\mathbf{q}\cdot(\mathbf{r}_t^j - \mathbf{r}_t^k)} \rangle$ [55,76], where the sum runs over all scatterers (atoms, particles, etc.). This also applies to interacting colloid suspensions, where $S(\mathbf{q})$ is the Fourier transform of the pair correlation function [55]. An even simpler observable is the radius of gyration, $R_g^2 \equiv (1/N)\sum_{j=1}^N \langle (\mathbf{r}_j - \bar{\mathbf{r}})^2 \rangle$ [11,55,77], where $\bar{\mathbf{r}} \equiv (1/N)\sum_{j=1}^N \mathbf{r}_j$ is the center of mass. R_g^2 reflects the (statistical) size of molecules and is easily inferred from small q via Guinier's law, $S(|\mathbf{q}|) \overset{|\mathbf{q}|\to 0}{=} S(0) e^{-|\mathbf{q}|^2 R_g^2/3}$ [55,77].

We consider the structure factor averaged over spatial dimensions $S(q)$ (see Ref. [62] for the vector version). For simplicity assume that γ is a known scalar. We observe how $S(q)$ changes over time. From Eq. (1) we can derive the bounds (see Ref. [62])

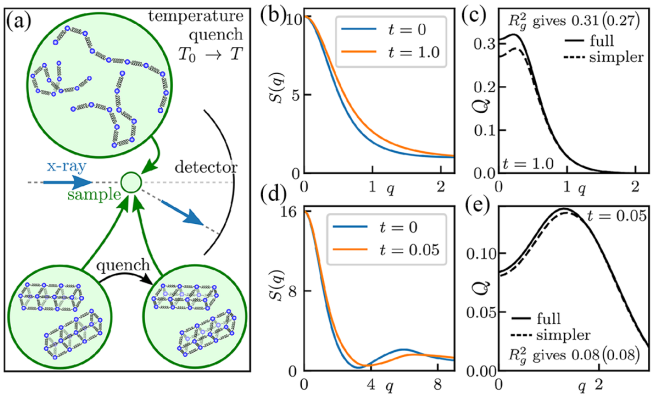

FIG. 2. (a) Sketch of a scattering setup with (b),(c) Rouse polymers with $N = 10$ beads subject to a temperature quench from $T_0 = 2T$ to T at $t = 0$, and (d),(e) harmonically confined "nanocrystal" with $N = 16$ with Hookean neighbor interactions subject to a quench in rest positions (see Ref. [62] for model details and parameters). (b),(d) Structure factors and (c),(e) corresponding quality factors [see Eq. (6); "simpler" bound contains $\max_\tau$ instead of integral].

$$T\Delta S_{\rm tot} \geq \frac{3\gamma[S_t(q) - S_0(q)]^2}{q^2 \int_0^t [N - S_\tau(2q)]d\tau} \geq \frac{3\gamma[S_t(q) - S_0(q)]^2}{q^2 t \max_\tau [N - S_\tau(2q)]}$$
$$T\Delta S_{\rm tot} \geq \frac{N[R_g^2(t) - R_g^2(0)]^2}{4\int_0^t d\tau R_g^2(\tau)/\gamma} \geq \frac{N[R_g^2(t) - R_g^2(0)]^2}{4t \max_\tau [R_g^2(\tau)]/\gamma}. \quad (6)$$

The second bound in each line is a simplification when the maximum over time is known, and it is not necessary to measure for all τ. The quality of these bounds for entropy production of internal degrees of freedom during relaxation is shown in Fig. 2 for a solution of (b),(c) Rouse polymers upon a temperature quench [see Figs. 2(b) and 2(c); probing, e.g., the thermal relaxation asymmetry [16,19,78]] and confined nanocrystals upon a structural transformation [see Figs. 2(d) and 2(e)], respectively. Dissipative processes occur on distinct length scales, leading to changes of $S_t(q)$ at distinct q [Figs. 2(b) and 2(d)]. In both cases, the sharpness of the bounds (6) depends on q, giving insight into the participation of distinct modes in dissipation. The q dependence can in turn be used for optimization of inference. For small q modes we recover the bound in terms of $R_g^2(\tau)$. We recover ~30% of $\Delta S_{\rm tot}$ in the quenched polymer solution and ~15% for the transforming nanocrystal. This is in fact a lot considering that we only measure a 1D projection of $3(N-1)$ internal degrees of freedom. Note that here the large contribution from low q modes is intuitive, since the temperature change mostly affects the overall statistical size of the polymer.

The bound (1) will be useful for many bulk experiments beyond scattering. Consider, for example, a bulk measurement of the mean FRET efficiency for a pair of donor and acceptor chromophores with Förster distance R_0 attached to some macromolecule, $E_t = \langle (1 + [(\mathbf{x}_t^{\rm don} - \mathbf{x}_t^{\rm acc})/R_0]^6)^{-1} \rangle$, where the simplest bound reads $T\Delta S_{\rm tot} \geq R_0^2 \gamma (E_t - E_0)^2/8t$ (for details see Ref. [62]).

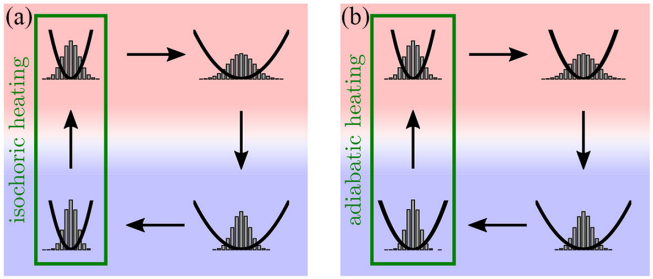

FIG. 3. Schematic of (a) a Stirling heat engine as realized in Ref. [79] and (b) a Carnot heat engine with adiabatic heating and cooling [85] as realized in Ref. [80]. Note that the stiffness is constant ("isochoric") during heating and cooling in (a) but *not* in (b). Red denotes hot and blue cold temperatures $T(\tau)$ of the environment (not to be confused with $T_{\rm p}$).

Example 3: Higher-order transport—Consider now a *centered* transient process x_τ, i.e., with constant mean $\langle x_t - x_0 \rangle = 0$. There is no mean transport. However, there is higher-order transport, in the simplest case $\langle x_t^2 - x_0^2 \rangle \neq 0$. Setting $z_\tau = x_\tau^2$ we then have $T\Delta S_{\rm tot} \geq \gamma \langle x_t^2 - x_0^2 \rangle^2 / 4\int_0^t d\tau \langle x_\tau^2 \rangle$. A concrete example is Brownian heat engines [79–81] in Fig. 3, where an "effective temperature" in a parabolic trap with stiffness $\kappa(\tau)$ is defined as $T_{\rm p}(\tau) \equiv \kappa(\tau)\langle x_\tau^2 \rangle / k_{\rm B}$ [81]. In this scenario, where the medium temperature varies in time, the left-hand side of the transport bound (1) becomes $T\Delta S_{\rm tot} \to \Delta(TS_{\rm tot}) \equiv \int_0^t d\tau T(\tau)\dot{S}_{\rm tot}(\tau)$, yielding [82]

$$\Delta(TS_{\rm tot}) \geq \frac{\left[T_{\rm p}(t) - T_{\rm p}(0) - \int_0^t T_{\rm p}(\tau)\frac{\partial_\tau \kappa(\tau)}{\kappa(\tau)} d\tau\right]^2}{4\int_0^t T_{\rm p}(\tau)\kappa(\tau)d\tau/k_{\rm B}\gamma}. \quad (7)$$

During an isochoric heating step ($\kappa =$ constant such that $\partial_\tau \kappa(\tau) = 0$) highlighted in Fig. 3(a), no work is performed [79], and the dissipation $\Delta(TS_{\rm tot})$ of an efficient engine should be minimal. Thus, to achieve a given $T_{\rm p}(t) - T_{\rm p}(0)$ [83] for minimal $\Delta(TS_{\rm tot})$, assuming that we can saturate the bound (as we can in the overdamped case), we either need long t or must maximize $\int_0^t d\tau T_{\rm p}(\tau)$, implying substantial heating at the beginning of the time interval $[0, t]$. For time-dependent $\kappa(\tau)$ [see Fig. 3(b) or the Carnot engine [80]], the bound in Eq. (7) is more complicated since *all* terms contribute when $\partial_\tau \kappa(\tau) \neq 0$. However, the bound still serves as a *fundamental* limit that can be evaluated for any given protocol. Note that the results equally apply to underdamped heat engines (as theoretically considered in, e.g., [84]).

Of mathematical interest for higher-order transport is the moment-generating function $\phi_\tau(\mathbf{q}) \equiv \langle e^{-\mathbf{q}\cdot\mathbf{x}_\tau} \rangle$, giving

$$T\Delta S_{\rm tot} \geq \frac{[\phi_t(\mathbf{q}) - \phi_0(\mathbf{q})]^2}{\int_0^t d\tau \phi_\tau(2\mathbf{q})\mathbf{q}^T\boldsymbol{\gamma}^{-1}(\tau)\mathbf{q}}, \quad (8)$$

which quantifies how changes of the qth mode of the probability density contribute to ΔS_{tot} and will be useful for proving future bounds.

Interpretation and handling of $\mathcal{D}^z(t)$—The interpretation of $\mathcal{D}^z(t)$ is intuitive: for a process $\mathbf{x}_\tau$ with given cost ΔS_{tot}, the transport $\langle z_t - z_0 \rangle$ will be larger for a function z that stretches $\mathbf{x}$ more. This stretching is rescaled by $\nabla_{\mathbf{x}} z$ in the quadratic form $\mathcal{D}^z(t)$ since ΔS_{tot} does *not* depend on z.

For simple marginal observations, $z(\mathbf{x}) = x_i$, we have that $\mathcal{D}^z = \boldsymbol{\gamma}_{ii}^{-1}$. Moreover, if we only observe z_τ but not $\mathbf{x}_\tau$, we can often bound $\mathcal{D}^z(t)$ in terms of $\langle z_\tau \rangle$ or in terms of constants, such as in the case of R_g^2 and $S_t(q)$ before (e.g., it suffices to know that z_τ has bounded derivatives). In the challenging case where we only observe z_τ but do not know the function $z(\mathbf{x})$ (i.e., it is some unknown projection or reaction coordinate), we can, given sufficient time resolution, determine or estimate $\mathcal{D}^z$ as follows: for overdamped dynamics we have $t\mathcal{D}^z(t) = \int_0^t d\tau \{\mathrm{var}[dz_\tau]/2k_{\mathrm{B}}T d\tau\}$ (for steady-state dynamics see Ref. [86], where $\mathcal{D}^z$ recently appeared in a correlation inequality). For underdamped dynamics, scalar m, γ, and $z_\tau = z(\mathbf{x}_\tau)$ (no explicit time dependence) we can obtain $\mathcal{D}^z(t)$ if we know the momentum relaxation time m/γ via $\{\mathrm{var}(d[(d/d\tau)z(\mathbf{x}_\tau)])/2k_{\mathrm{B}}T dt\} = (\gamma^2/m^2)\langle \gamma^{-1}[\nabla_{\mathbf{x}} z(\mathbf{x}_\tau)]^2 \rangle$. If the system relaxes to equilibrium we can obtain γ/m from observations of z_τ via equilibrium measurements of $\mathrm{var}(d[(d/d\tau)z(\mathbf{x}_\tau)])$ and $\mathrm{var}[dz(\mathbf{x}_\tau)]$ (see Ref. [62]). If the system relaxes to a NESS, we can upper bound $\mathcal{D}^z$ by using that $m/\gamma \leq t_{\mathrm{rel}}$ with the relaxation time of the system determined, e.g., from correlation functions $t_{\mathrm{rel}}^{-1} = -\lim_{t\to\infty} t^{-1} \ln[\langle z_t z_0 \rangle - \langle z_t \rangle \langle z_0 \rangle]$ (see Ref. [62]).

Conclusion—We proved an inequality upper-bounding transport of any differentiable scalar observable in a general d-dimensional nonequilibrium system in terms of the total entropy production and fluctuation-scale function that "corrects" for the amount the observation stretches microscopic coordinates. We explained how to saturate the bound. The result, classifiable as a time-integrated generalized speed limit, may be understood as a thermodynamic cost of transport of observables and allows for inferring a lower bound on dissipation, thus complementing the TUR and existing speed limits. The bound places underdamped and overdamped stochastic as well as deterministic systems on equal footing. This fills an important gap, because microscopic dynamics is—at least on short timescales—underdamped, and the TUR does not hold for underdamped dynamics. In particular short-time TURs for overdamped dynamics [29,30,87] are expected to fail.

By only requiring averages, the transport bound is statistically less demanding and applicable to both single-molecule as well as bulk experiments. This is attractive in the context of time-resolved x-ray scattering on biomolecules, as it will allow thermodynamic inference from bulk observations of controlled transients [72–75]. This may facilitate thermodynamic inference on molecular machines without an obvious directionality such molecular chaperones [60], which remains challenging even with most advanced single-molecule techniques [61]. The bound allows for versatile applications and generalizations to vectorial observables $\mathbf{z}$ and adaptations for Markov-jump dynamics.

Acknowledgments—Financial support from the European Research Council (ERC) under the European Union's orizon Europe research and innovation program (Grant Agreement No. 101086182 to A. G.) is gratefully acknowledged.

[1] U. Seifert, Stochastic thermodynamics, fluctuation theorems and molecular machines, Rep. Prog. Phys. **75**, 126001 (2012).
[2] U. Seifert, Entropy production along a stochastic trajectory and an integral fluctuation theorem, Phys. Rev. Lett. **95**, 040602 (2005).
[3] U. Seifert, Stochastic thermodynamics: From principles to the cost of precision, Physica (Amsterdam) **504A**, 176 (2018).
[4] M. P. Leighton and D. A. Sivak, Dynamic and thermodynamic bounds for collective motor-driven transport, Phys. Rev. Lett. **129**, 118102 (2022).
[5] M. P. Leighton and D. A. Sivak, Inferring subsystem efficiencies in bipartite molecular machines, Phys. Rev. Lett. **130**, 178401 (2023).
[6] I. Di Terlizzi, M. Gironella, D. Herraez-Aguilar, T. Betz, F. Monroy, M. Baiesi, and F. Ritort, Variance sum rule for entropy production, Science **383**, 971 (2024).
[7] D. Sato, T. Hikima, and M. Ikeguchi, Time-resolved small-angle x-ray scattering of protein cage assembly, in *Protein Cages. Methods in Molecular Biology* (Springer, New York, 2023), p. 211, Vol. 2671, 10.1007/978-1-0716-3222-2_12.
[8] M. Roessle, E. Manakova, I. Lauer, T. Nawroth, J. Holzinger, T. Narayanan, S. Bernstorff, H. Amenitsch, and H. Heumann, Time-resolved small angle scattering: Kinetic and structural data from proteins in solution, J. Appl. Crystallogr. **33**, 548 (2000).
[9] S. Akiyama, S. Takahashi, T. Kimura, K. Ishimori, I. Morishima, Y. Nishikawa, and T. Fujisawa, Conformational landscape of cytochrome c folding studied by microsecond-resolved small-angle x-ray scattering, Proc. Natl. Acad. Sci. U.S.A. **99**, 1329 (2002).
[10] J. Stamatoff, An approach for time-resolved x-ray scattering, Biophys. J. **26**, 325 (1979).
[11] Y. Yamada, T. Matsuo, H. Iwamoto, and N. Yagi, A compact intermediate state of calmodulin in the process of target binding, Biochemistry **51**, 3963 (2012).
[12] H. S. Cho, F. Schotte, V. Stadnytskyi, and P. Anfinrud, Time-resolved x-ray scattering studies of proteins, Curr. Opin. Struct. Biol. **70**, 99 (2021).
[13] D. Arnlund *et al.*, Visualizing a protein quake with time-resolved x-ray scattering at a free-electron laser, Nat. Methods **11**, 923 (2014).
[14] H. S. Cho, N. Dashdorj, F. Schotte, T. Graber, R. Henning, and P. Anfinrud, Protein structural dynamics in solution

unveiled via 100-ps time-resolved x-ray scattering, Proc. Natl. Acad. Sci. U.S.A. **107**, 7281 (2010).
[15] M. Cammarata, M. Levantino, F. Schotte, P. A. Anfinrud, F. Ewald, J. Choi, A. Cupane, M. Wulff, and H. Ihee, Tracking the structural dynamics of proteins in solution using time-resolved wide-angle x-ray scattering, Nat. Methods **5**, 881 (2008).
[16] M. Ibáñez, C. Dieball, A. Lasanta, A. Godec, and R. A. Rica, Heating and cooling are fundamentally asymmetric and evolve along distinct pathways, Nat. Phys. **20**, 135 (2024).
[17] J. L. Lebowitz and P. G. Bergmann, Irreversible Gibbsian ensembles, Ann. Phys. (N.Y.) **1**, 1 (1957).
[18] S. Vaikuntanathan and C. Jarzynski, Dissipation and lag in irreversible processes, Europhys. Lett. **87**, 60005 (2009).
[19] A. Lapolla and A. Godec, Faster uphill relaxation in thermodynamically equidistant temperature quenches, Phys. Rev. Lett. **125**, 110602 (2020).
[20] Z. T. Berndsen, N. Keller, S. Grimes, P. J. Jardine, and D. E. Smith, Nonequilibrium dynamics and ultraslow relaxation of confined DNA during viral packaging, Proc. Natl. Acad. Sci. U.S.A. **111**, 8345 (2014).
[21] H. Turlier, D. A. Fedosov, B. Audoly, T. Auth, N. S. Gov, C. Sykes, J.-F. Joanny, G. Gompper, and T. Betz, Equilibrium physics breakdown reveals the active nature of red blood cell flickering, Nat. Phys. **12**, 513 (2016).
[22] T. Stuchinskaya, L. A. Mitchenall, A. J. Schoeffler, K. D. Corbett, J. M. Berger, A. D. Bates, and A. Maxwell, How do type II topoisomerases use ATP hydrolysis to simplify DNA topology beyond equilibrium? Investigating the relaxation reaction of nonsupercoiling type II topoisomerases, J. Mol. Biol. **385**, 1397 (2009).
[23] J. Gieseler and J. Millen, Levitated nanoparticles for microscopic thermodynamics–a review, Entropy **20**, 326 (2018).
[24] A. C. Barato and U. Seifert, Thermodynamic uncertainty relation for biomolecular processes, Phys. Rev. Lett. **114**, 158101 (2015).
[25] T. R. Gingrich, J. M. Horowitz, N. Perunov, and J. L. England, Dissipation bounds all steady-state current fluctuations, Phys. Rev. Lett. **116**, 120601 (2016).
[26] T. R. Gingrich, G. M. Rotskoff, and J. M. Horowitz, Inferring dissipation from current fluctuations, J. Phys. A **50**, 184004 (2017).
[27] T. Van Vu and Y. Hasegawa, Uncertainty relations for underdamped Langevin dynamics, Phys. Rev. E **100**, 032130 (2019).
[28] J. M. Horowitz and T. R. Gingrich, Thermodynamic uncertainty relations constrain non-equilibrium fluctuations, Nat. Phys. **16**, 15 (2019).
[29] S. K. Manikandan, D. Gupta, and S. Krishnamurthy, Inferring entropy production from short experiments, Phys. Rev. Lett. **124**, 120603 (2020).
[30] S. Otsubo, S. Ito, A. Dechant, and T. Sagawa, Estimating entropy production by machine learning of short-time fluctuating currents, Phys. Rev. E **101**, 062106 (2020).
[31] K. Liu, Z. Gong, and M. Ueda, Thermodynamic uncertainty relation for arbitrary initial states, Phys. Rev. Lett. **125**, 140602 (2020).
[32] T. Koyuk and U. Seifert, Thermodynamic uncertainty relation for time-dependent driving, Phys. Rev. Lett. **125**, 260604 (2020).
[33] C. Dieball and A. Godec, Mathematical, thermodynamical, and experimental necessity for coarse graining empirical densities and currents in continuous space, Phys. Rev. Lett. **129**, 140601 (2022).
[34] C. Dieball and A. Godec, Coarse graining empirical densities and currents in continuous-space steady states, Phys. Rev. Res. **4**, 033243 (2022).
[35] A. Dechant and S.-I. Sasa, Continuous time reversal and equality in the thermodynamic uncertainty relation, Phys. Rev. Res. **3**, L042012 (2021).
[36] A. Dechant and S.-I. Sasa, Improving thermodynamic bounds using correlations, Phys. Rev. X **11**, 041061 (2021).
[37] C. Dieball and A. Godec, Direct route to thermodynamic uncertainty relations and their saturation, Phys. Rev. Lett. **130**, 087101 (2023).
[38] K. Brandner, K. Saito, and U. Seifert, Strong bounds on Onsager coefficients and efficiency for three-terminal thermoelectric transport in a magnetic field, Phys. Rev. Lett. **110**, 070603 (2013).
[39] N. Shiraishi, K. Funo, and K. Saito, Speed limit for classical stochastic processes, Phys. Rev. Lett. **121**, 070601 (2018).
[40] N. Shiraishi and K. Saito, Information-theoretical bound of the irreversibility in thermal relaxation processes, Phys. Rev. Lett. **123**, 110603 (2019).
[41] G. Falasco and M. Esposito, Dissipation-time uncertainty relation, Phys. Rev. Lett. **125**, 120604 (2020).
[42] K. Yoshimura and S. Ito, Thermodynamic uncertainty relation and thermodynamic speed limit in deterministic chemical reaction networks, Phys. Rev. Lett. **127**, 160601 (2021).
[43] E. Aurell, C. Mejía-Monasterio, and P. Muratore-Ginanneschi, Optimal protocols and optimal transport in stochastic thermodynamics, Phys. Rev. Lett. **106**, 250601 (2011).
[44] E. Aurell, K. Gawedzki, C. Mejía-Monasterio, R. Mohayaee, and P. Muratore-Ginanneschi, Refined second law of thermodynamics for fast random processes, J. Stat. Phys. **147**, 487–505 (2012).
[45] E. Potanina, C. Flindt, M. Moskalets, and K. Brandner, Thermodynamic bounds on coherent transport in periodically driven conductors, Phys. Rev. X **11**, 021013 (2021).
[46] A. Dechant and S.-I. Sasa, Entropic bounds on currents in Langevin systems, Phys. Rev. E **97**, 062101 (2018).
[47] S. Ito and A. Dechant, Stochastic time evolution, information geometry, and the Cramér-Rao bound, Phys. Rev. X **10**, 021056 (2020).
[48] T. Van Vu and K. Saito, Thermodynamic unification of optimal transport: Thermodynamic uncertainty relation, minimum dissipation, and thermodynamic speed limits, Phys. Rev. X **13**, 011013 (2023).
[49] P. Pietzonka, Classical pendulum clocks break the thermodynamic uncertainty relation, Phys. Rev. Lett. **128**, 130606 (2022).
[50] L. P. Fischer, H.-M. Chun, and U. Seifert, Free diffusion bounds the precision of currents in underdamped dynamics, Phys. Rev. E **102**, 012120 (2020).

[51] C. Kwon and H. K. Lee, Thermodynamic uncertainty relation for underdamped dynamics driven by time-dependent protocols, New J. Phys. **24**, 013029 (2022).

[52] R.-S. Fu and T. R. Gingrich, Thermodynamic uncertainty relation for Langevin dynamics by scaling time, Phys. Rev. E **106**, 024128 (2022).

[53] S. Lee, D.-K. Kim, J.-M. Park, W. K. Kim, H. Park, and J. S. Lee, Multidimensional entropic bound: Estimator of entropy production for Langevin dynamics with an arbitrary time-dependent protocol, Phys. Rev. Res. **5**, 013194 (2023).

[54] J. Lyu, K. J. Ray, and J. P. Crutchfield, Entropy production by underdamped Langevin dynamics, arXiv:2405.12305.

[55] J. K. G. Dhont, *An Introduction to Dynamics of Colloids*, Studies in Interface Science (Elsevier, New York, 1996).

[56] J. A. McCammon, Protein dynamics, Rep. Prog. Phys. **47**, 1 (1984).

[57] J. C. Smith, Protein dynamics: Comparison of simulations with inelastic neutron scattering experiments, Q. Rev. Biophys. **24**, 227 (1991).

[58] G. R. Kneller, Inelastic neutron scattering from damped collective vibrations of macromolecules, Chem. Phys. **261**, 1 (2000).

[59] F. N. Brünig, J. O. Daldrop, and R. R. Netz, Pair-reaction dynamics in water: Competition of memory, potential shape, and inertial effects, J. Phys. Chem. B **126**, 10295 (2022).

[60] A. Mashaghi, G. Kramer, D. C. Lamb, M. P. Mayer, and S. J. Tans, Chaperone action at the single-molecule level, Chem. Rev. **114**, 660 (2013).

[61] C. Ratzke, B. Hellenkamp, and T. Hugel, Four-colour fret reveals directionality in the Hsp90 multicomponent machinery, Nat. Commun. **5**, 4192 (2014).

[62] See Supplemental Material at http://link.aps.org/supplemental/10.1103/PhysRevLett.133.067101, which includes Refs. [63–66] for derivations, further examples, and details.

[63] A. Dechant, Minimum entropy production, detailed balance and Wasserstein distance for continuous-time Markov processes, J. Phys. A **55**, 094001 (2022).

[64] C. W. Gardiner, *Handbook of Stochastic Methods for Physics, Chemistry, and the Natural Sciences*, 2nd ed. (Springer-Verlag, Berlin, New York, 1985).

[65] S. Pigolotti, I. Neri, É. Roldán, and F. Jülicher, Generic properties of stochastic entropy production, Phys. Rev. Lett. **119**, 140604 (2017).

[66] A. Dechant and S.-I. Sasa, Current fluctuations and transport efficiency for general Langevin systems, J. Stat. Mech. (2018) 063209.

[67] J.-D. Benamou and Y. Brenier, A computational fluid mechanics solution to the Monge-Kantorovich mass transfer problem, Numer. Math. **84**, 375 (2000).

[68] I. Josts, Y. Gao, D. C. Monteiro, S. Niebling, J. Nitsche, K. Veith, T. W. Gräwert, C. E. Blanchet, M. A. Schroer, N. Huse, A. R. Pearson, D. I. Svergun, and H. Tidow, Structural kinetics of MsbA investigated by stopped-flow time-resolved small-angle x-ray scattering, Structure **28**, 348 (2020).

[69] H. Risken, *The Fokker-Planck Equation* (Springer Berlin Heidelberg, Berlin, Heidelberg, 1989).

[70] G. Wilemski, On the derivation of Smoluchowski equations with corrections in the classical theory of Brownian motion, J. Stat. Phys. **14**, 153 (1976).

[71] A. C. Barato and U. Seifert, Cost and precision of Brownian clocks, Phys. Rev. X **6**, 041053 (2016).

[72] K. Dave and M. Gruebele, Fast-folding proteins under stress, Cell Mol. Life Sci. **72**, 4273 (2015).

[73] J. Woenckhaus, R. Köhling, P. Thiyagarajan, K. C. Littrell, S. Seifert, C. A. Royer, and R. Winter, Pressure-jump small-angle x-ray scattering detected kinetics of staphylococcal nuclease folding, Biophys. J. **80**, 1518 (2001).

[74] J. Kubelka, Time-resolved methods in biophysics. 9. Laser temperature-jump methods for investigating biomolecular dynamics, Photochem. Photobiol. Sci. **8**, 499 (2009).

[75] B. Vestergaard, M. Groenning, M. Roessle, J. S. Kastrup, M. v. de Weert, J. M. Flink, S. Frokjaer, M. Gajhede, and D. I. Svergun, A helical structural nucleus is the primary elongating unit of insulin amyloid fibrils, PLoS Biol. **5**, e134 (2007).

[76] C. Dieball, D. Krapf, M. Weiss, and A. Godec, Scattering fingerprints of two-state dynamics, New J. Phys. **24**, 023004 (2022).

[77] D. I. Svergun and M. H. J. Koch, Small-angle scattering studies of biological macromolecules in solution, Rep. Prog. Phys. **66**, 1735 (2003).

[78] C. Dieball, G. Wellecke, and A. Godec, Asymmetric thermal relaxation in driven systems: Rotations go opposite ways, Phys. Rev. Res. **5**, L042030 (2023).

[79] V. Blickle and C. Bechinger, Realization of a micrometre-sized stochastic heat engine, Nat. Phys. **8**, 143 (2011).

[80] I. A. Martínez, É. Roldán, L. Dinis, D. Petrov, J. M. R. Parrondo, and R. A. Rica, Brownian Carnot engine, Nat. Phys. **12**, 67 (2015).

[81] I. A. Martínez, E. Roldán, L. Dinis, and R. A. Rica, Colloidal heat engines: A review, Soft Matter **13**, 22 (2017).

[82] Alternatively we can also derive a bound for ΔS_{tot} but we opt for $\Delta(TS_{\mathrm{tot}})$ for a "direct" energetic interpretation.

[83] More precisely, a given $\gamma[T_{\mathrm{p}}(t) - T_{\mathrm{p}}(0)]^2/\kappa$.

[84] A. Dechant, N. Kiesel, and E. Lutz, Underdamped stochastic heat engine at maximum efficiency, Europhys. Lett. **119**, 50003 (2017).

[85] I. A. Martínez, E. Roldán, L. Dinis, D. Petrov, and R. A. Rica, Adiabatic processes realized with a trapped Brownian particle, Phys. Rev. Lett. **114**, 120601 (2015).

[86] A. Dechant, J. Garnier-Brun, and S.-I. Sasa, Thermodynamic bounds on correlation times, Phys. Rev. Lett. **131**, 167101 (2023).

[87] S. Otsubo, S. K. Manikandan, T. Sagawa, and S. Krishnamurthy, Estimating time-dependent entropy production from non-equilibrium trajectories, Commun. Phys. **5**, 11 (2022).